Contemporary Mathematics
https://ojs.wiserpub.com/index.php/CM/

Research Article

A Deterministic Approach to Quantifying Hearing Temporary Threshold Shift

Tichaona Chikore[1], **Farai Nyabadza**[1,2*]

[1] Department of Applied Mathematics, University of Johannesburg, South Africa
[2] Institute of Applied Research and Technology, Emirates Aviation University, Dubai International Academic City, UAE
E-mail: fnyabadza@uj.ac.za

Received: 15 January 2025; **Revised:** 24 March 2025; **Accepted:** 1 April 2025

Abstract: This study investigates the dynamics of cochlear hair cell populations under environmental stressors such as prolonged exposure to loud noise from earphones. To understand potential temporary hearing loss dynamics due to earphones, a mathematical model is developed in this investigation to capture the behavior of healthy, fatigued, and impaired hair cells in response to varying sound intensities, described by differential equations incorporating sound intensity and its regulation. The model is scaled and analysis of the system's steady states show that two endemic equilibria exist, with local asymptotic stability investigated using the Jacobian matrix. Results show that there is a critical level of sound exposure above which the auditory system can no longer maintain a healthy state, leading to long-term hearing impairment. Simulation results show that for a given intensity level, hearing loss is inevitable for certain for specific Temporary Threshold Shift (TTS). We are able to quantify healthy and acceptable TTS levels, beyond which there are no healthy, fatigued or impaired hair cells. The results can be used to predict hearing impairment outcomes and guide evidence-based interventions to mitigate the adverse effects of prolonged low-pressure sound exposure on auditory health.

***Keywords*:** hair cells, noise-induced hearing loss, Temporary Threshold Shift (TTS), fatigue, cochlear damage, impairment

MSC: 92B20, 34D20, 92C50

Abbreviation

TTS	Temporary Threshold Shift
NIHL	Noise-Induced Hearing Loss

1. Introduction

Hearing loss is a significant health issue worldwide, influenced by multiple factors that lead to its development and worsening. While the impact of loud noises on hearing is well-known, there is growing interest in understanding the effects of long-term exposure to low-level sounds [1]. Unlike high-volume sounds that can cause immediate harm to the auditory system, continuous exposure to lower sound levels poses a different but noteworthy threat to hearing [2, 3]. This

DOI: https://doi.org/10.37256/cm.6420256435

situation emphasizes the intricate relationship between sound stimuli and the auditory system's physiological responses. To devise effective prevention and intervention strategies, it is essential to comprehend how prolonged exposure to low-pressure sounds causes hearing damage, with particular focus on the hair cells. A fundamental concept in this area is Temporary Threshold Shift (TTS) [4], where hair cells become overworked and swollen, resulting in diminished auditory function and a sensation of muffled hearing [5]. Although TTS can often reverse, repeated exposure can lead to long-term hearing issues such as tinnitus (hearing sounds that are not being generated by an external environmental source [6]) have and challenges in understanding speech in noisy settings [7]. Figure 1 that follows illustrates the different noise exposures and their effects.

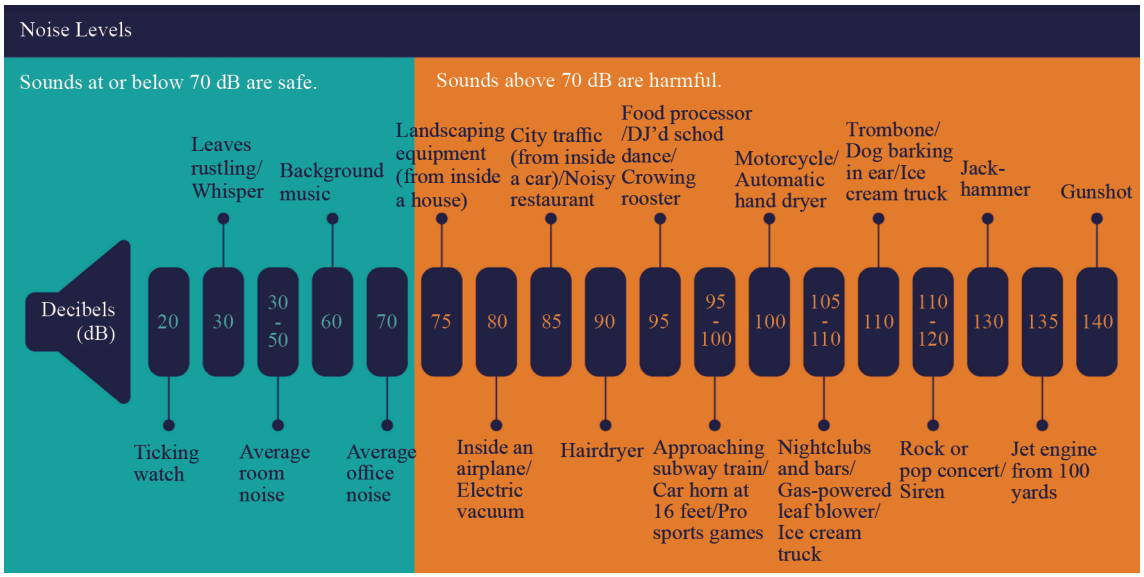

Figure 1. Noise-Induced Hearing Loss (NIHL) depiction courtesy of [1]

The use of earphones has become ubiquitous in modern society, raising concerns about its potential impact on hearing health. Studies have shown that prolonged use of earphones at high volumes can lead to Noise-Induced Hearing Loss (NIHL). A study in [8] highlights that listening to music through earphones at levels exceeding 85 decibels for extended periods can damage hair cells in the cochlea, leading to permanent hearing loss. Earphones contribute to TTS and the risk is further compounded by the use of earphones in noisy environments, where users may increase the volume to overcome background noise (masking), thereby exceeding safe listening levels [9].

Other studies have shown that the type of earphones used can influence the degree of hearing risk. For instance, circumaural headphones, which cover the entire ear, generally pose less risk compared to in-ear models because they can provide better sound isolation, reducing the need for higher volumes [10]. Many users of portable music players tend to set the volume at levels that pose a risk for NIHL, especially when using earphones that insert directly into the ear canal [11]. Nonetheless, regardless of the type, it is crucial for users to adopt safe listening practices, such as following the 60/60 rule —listening at no more than 60% of maximum volume for no longer than 60 minutes at a time [12]. Implementing these precautions can help mitigate the adverse effects of earphone use on hearing health and ensure a safer listening experience. To gain further understanding of the hearing loss dynamics, we formulate mathematical formalization of how the process of hearing loss unfolds due to exposure to toxic sounds, as time progresses using ordinary differential equations.

This paper presents a mathematical overview of the impact of prolonged low-pressure sound exposure on hearing health, incorporating insights from acoustics, physiology, and mathematical studies. The main drive of this study is the foundational understanding that damage to hair cells due to exposure to loud sounds (see also [13]) is pivotal in inducing hearing loss. The study seeks to predict and quantify how hearing loss propagates by determining tolerable persistent

sound intensity thresholds by considering the hair cells as population in various states depending on the nature of the exposure to provide a framework for predicting hearing impairment outcomes, understanding the hearing loss dynamics, and guiding evidence-based interventions to mitigate the adverse effects of prolonged low-pressure sound exposure on auditory health.

The paper is structured as follows: In Section 1 we have the introduction followed by the model formulation in Section 2 where stability analysis of steady states, positivity and boundedness of solutions among other analysis are undertaken. The model results and simulations are in Section 3 and the discussion and conclusion in Section 4.

2. The model

The model describes how cochlear hair cells, crucial for auditory function, respond to environmental stressors like prolonged exposure to loud noise from earphones. It considers three main populations of hair cells: healthy cells, which guarantee effective hearing (X); fatigued, which are still functional but have undergone some stress (Y); and impaired cells that have reversibly lost their function (Z). The hair cell populations behave dynamically under the influence of sound intensity represented as I, which captures the detrimental effect of earphone use. The environment noise gives the baseline sound intensity and is denoted by I_b, and sound intensity adjusts towards the baseline at a rate α. Recovery rate of healthy cells from the fatigued and impaired state is represented by Λ. Healthy cells become impaired (skipping fatigue state) at a rate γ, reflecting instant temporary but harmful damage. Conversion of healthy cells to fatigued cells happens at a rate β_1. Fatigued cells Y can arise from two main sources: they can either directly result from the conversion of healthy cells under the influence of I, or they can revert from an impaired cells state Z back to fatigued due to the inconsistent prevalence of sound intensity at a rate β_2. The rate of change in the sound intensity is also driven by the source's sound intensity capabilities, with a maximum intensity I_{max}, and this is represented by the Holling Type 2 response function $\frac{\lambda I}{1+\varepsilon I}$, where ε quantifies the intensity distribution. Fatigued cells decay over time and transition further to an impaired state Z at a rate σ. In each state, hair cells decrease naturally over time due to decay rate δ as a result of failure by some hair cells to regenerate or persistent stress. Thus, we get the model system:

$$\begin{aligned}
\frac{dX}{dt} &= \Lambda - \beta_1 XI - (\gamma+\delta)X,\\
\frac{dY}{dt} &= \beta_1 XI + \beta_2 YI - (\delta+\sigma)Y,\\
\frac{dZ}{dt} &= \gamma X + \sigma Y - \beta_2 YI - \delta Z,\\
\frac{dI}{dt} &= \alpha(I_b - I) + \frac{\lambda I}{1+\varepsilon I}
\end{aligned} \tag{1}$$

We assume that all the parameters are non-negative, and that the system is governed by the initial conditions $X(0) \geq 0$, $Y(0) \geq 0$, $Z(0) \geq 0$, and $I(0) \geq 0$. The scaled system for the model system (1) is obtained by setting

$$u = \frac{X}{N},\ v = \frac{Y}{N},\ w = \frac{Z}{N},\ r = \frac{I}{I_{max}} \text{ and } \tau = \alpha t,$$

and without loss of generality, we set $\tau = t$ to get the model system:

$$\begin{aligned}
\frac{du}{dt} &= \alpha_1 - \alpha_2 ur - \alpha_0 u - \alpha_3 u, \\
\frac{dv}{dt} &= \alpha_2 ur + \alpha_4 wr - (\alpha_3 + \alpha_5)v, \\
\frac{dw}{dt} &= \alpha_0 u + \alpha_5 v - \alpha_4 rw - \alpha_3 w, \\
\frac{dr}{dt} &= \alpha_6 - r + \frac{\alpha_7 r}{1 + \alpha_8 r}.
\end{aligned} \tag{2}$$

We define the non-negative parameters $\alpha_0 = \frac{\gamma}{\alpha}$, $\alpha_1 = \frac{\Lambda}{N\alpha}$, $\alpha_2 = \frac{\beta_1 N}{\alpha}$, $\alpha_3 = \frac{\delta}{\alpha}$, $\alpha_4 = \frac{\beta_2 N}{\alpha}$, $\alpha_5 = \frac{\sigma}{\alpha}$, $\alpha_6 = \frac{\sigma}{\alpha}$, $\alpha_6 = \frac{I_b}{I_{max}}$, $\alpha_7 = \frac{\lambda}{\gamma}$ and $\alpha_8 = \varepsilon I_{max}$. We proceed to show that the scaled model system (2) has positive and bounded solutions.

We define the parameter groups $\alpha_{3,5,7}$ as follows:

• The first level (from X to Y) Impairment-Incidence Ratio (IIR_1) represents the lethality of the sound intensity that leads to hair cell fatigue, and is denoted by α_3.

• The second level (from Y to Z) Impairment-Incidence Ratio (IIR_2) represents the lethality of the sound intensity that leads to hair cells impairment, and is denoted by α_5.

• The Temporary Threshold Shift (TTS) factor is denoted by α_7.

2.1 *Model properties*

The key attributes of the model such as positivity and boundedness of solutions are discussed in the sequel.

2.1.1 *Positivity and boundedness of solutions*

Theorem 1 For all $t \geq 0$, the model system (2) equipped with a solution set Δ and initial values $u \geq 0$, $v \geq 0$, $w \geq 0$, and $r \geq 0$, then we have that the solution components of Δ are non-negative and have complete boundedness.

Proof. Given that all of the initial conditions are positive, the first differential equation of (2) yields

$$\frac{du}{dt} + (\alpha_0 + \alpha_2 r + \alpha_3)u \geq 0, \tag{3}$$

where after calculus of integration, we get that

$$u(t) \geq u(0)e^{-\left(\alpha_2(\alpha_0+\alpha_3)t + \int_0^t r(\tau)d\tau\right)} > 0, \qquad \forall t > 0.$$

The solution $s(t)$ is guaranteed to remain positive for all $t \geq 0$ since the exponential function is always positive since the initial value $u(0) \geq 0$. Considering the second equation of model system (2) we have that:

$$\frac{dv}{dt} + (\alpha_3 + \alpha_5)v \geq 0,$$

from which we get the solution

$$v(t) \geq v(0)e^{-(\alpha_3+\alpha_5)t} > 0, \qquad \forall t > 0.$$

The solution $v(t)$ is guaranteed to remain positive for all $t \geq 0$ since the exponential function is always positive since the initial value $v(0) \geq 0$. From the third differential equation, we get that

$$\frac{dw}{dt} + (\alpha_4 r + \alpha_3)w \geq 0,$$

from which we get the solution

$$w(t) \geq w(0)e^{-(\alpha_3 t+\alpha_4 \int_0^t r(\tau)d\tau)t} > 0, \qquad \forall t > 0.$$

The solution $w(t)$ is guaranteed to remain positive for all $t \geq 0$ since the exponential function is always positive since the initial value $w(0) \geq 0$. The fourth differential equation gives

$$\frac{dr}{dt} + r \geq 0,$$

from which we get the solution

$$r(t) \geq r(0)e^{-t} > 0, \qquad \forall t > 0.$$

Similarly, the solution $r(t)$ is guaranteed to remain positive for all $t \geq 0$ since the exponential function is always positive since the initial value $r(0) \geq 0$. □

2.2 *Invariant region*

The system (2) is examined within the biologically relevant domain, Ω. Since the model tracks variations in the population of hair cells, it is crucial that all variables and parameters remain positive for all $t \geq 0$.

Theorem 2 With respect to system (2), the feasible region Ω defined by

$$\Omega = \{u, v, w \geq 0 : u + v + w = 1\}$$

is bounded, positively invariant and attracting for all $t > 0$.

Proof. We observe that

$$n(t) = u(t) + v(t) + w(t),$$

such that

$$\frac{dn}{dt} = \frac{du}{dt} + \frac{dv}{dt} + \frac{dw}{dt}.$$

We sum the differential equations:

$$\begin{aligned}\frac{dn}{dt} &= \frac{du}{dt} + \frac{dv}{dt} + \frac{dw}{dt} \\ &= \alpha_1 - \alpha_3(u+v+w) \\ &= \alpha_1 - \alpha_3 n(t).\end{aligned}$$

Grouping similar terms gives:

$$\frac{dn}{dt} = (\alpha_1 + \alpha_8) - (\alpha_3 u + \alpha_5 v + \alpha_6 v + \alpha_7 w + \alpha_9 r) + u.$$

Since all parameters $\alpha_i \geq 0$ and all variables u, v, w, $r \geq 0$, we have:

$$\frac{dn}{dt} \leq \alpha_1 + \alpha_3 n(t).$$

Integrating this inequality with respect to t gives:

$$n(t) \leq \frac{\alpha_1}{\alpha_3} - \left(\frac{\alpha_1}{\alpha_3} - n(0)\right) e^{-\alpha_3 t},$$

where $n(0)$ is the initial value of the total population $n(t)$. This shows that $n(t)$ is bounded for all $t \geq 0$. Hence, the solutions $u(t)$, $v(t)$, $w(t)$, and $r(t)$ of the system are bounded for all $t \geq 0$. We denote the feasible region by Ω such that

$$\Omega = \{u(t), v(t), w(t) \in \mathbb{R}^3 | u(t) + v(t) + w(t) \leq n(t) \leq 1\}.$$

Moreover, we have that $\lim_{x\to\infty} \sup n(t) \leq \frac{\alpha_1}{\alpha_3}$. Thus, for the model system (2), there exists a positively invariant region Ω such that Ω is a well-posed region for the system given by (2). □

2.3 *Stability analysis*

We show that the system has two endemic steady-states. We determine the conditions for the existence and local stability of the steady-states through the Jacobian matrix.

2.3.1 *The steady-states and local stability*

Setting the derivatives in the model system (2) to zero, we identify the steady state solutions $E_{1,2} = (u^*, v^*, w^*, r^*)$ such that:

$$E_{1,2} = \left(\begin{array}{c} \dfrac{\alpha_1}{\alpha_3 + \alpha_2 K_{1,2} + 1}, \ \dfrac{\alpha_1 \left(\alpha_2 \alpha_4 (K_{1,2})^2 + \alpha_2 \alpha_3 K_{1,2} + \alpha_4 K_{1,2}\right)}{\alpha_3 \left(\alpha_3 + \alpha_2 K_{1,2} + 1\right)\left(\alpha_3 + \alpha_5 + \alpha_4 K_{1,2}\right)}, \\ \\ \dfrac{\alpha_1 \left(\alpha_3 + \alpha_5 + \alpha_2 \alpha_5 K_{1,2}\right)}{\alpha_3 \left(\alpha_3 + \alpha_2 K_{1,2} + 1\right)\left(\alpha_3 + \alpha_5 + \alpha_4 K_{1,2}\right)}, \ K_{1,2} \end{array} \right), \tag{4}$$

where $K_{1,2}$ represents the two solutions to the quadratic equation

$$\alpha_9 r^2 + r(1 - R_i) - \kappa = 0 \tag{5}$$

which is of the form $a_1 r^2 + a_2 r + a_3 = 0$ with $R_i = \alpha_6 \alpha_8 + \alpha_7$, the relative intensity, measuring how the current sound intensity compares to the baseline and $\kappa = \alpha_6$, a constant. The quadratic equation yields the solution

$$K_{1,2} = \frac{-a_2 \pm \sqrt{a_2^2 + 4a_1 a_3}}{2a_1}. \tag{6}$$

Noting the quadratic formula above, by simple inspection of the discriminant and observing that it is greater than zero always, we have two positive solutions for the quadratic equation (5), on condition that $R_i > 1$. Hence, there are two endemic steady states if $R_i > 1$ and the Jacobian matrix of the model system is given as

$$J_{(E_1, E_2)} = \left(\begin{array}{cccc} -K_{1,2}\alpha_2 - \alpha_3 - 1 & 0 & 0 & -\alpha_2 u \\ K_{1,2}\alpha_2 & -\alpha_3 - \alpha_5 & K_{1,2} & \alpha_4 w \\ 1 & \alpha_5 & -\alpha_3 - K_{1,2}\alpha_4 & -\alpha_4 w \\ 0 & 0 & 0 & \dfrac{-\alpha_9 \alpha_8}{(1 + \alpha_9 w)^2} - \alpha_7 \end{array} \right) \tag{7}$$

We get the set of eigenvalues Λ such that

$$\Lambda_{(J_1, J_2)} = \left(-\alpha_3, \ -\alpha_3 - \alpha_2 K_{1,2} - 1, \ -\alpha_3 - \alpha_5 - \alpha_4 K_{1,2}, \ \frac{-\alpha_8 \alpha_9 - \alpha_7 - \alpha_7 \alpha_9^2 (K_{1,2})^2 - 2\alpha_7 \alpha_9 K_{1,2}}{(\alpha_9 K_{1,2} + 1)^2} \right).$$

Consequently, we state the following result whose proof is obvious by observing the nature of set $\Lambda_{(J_1, J_2)}$:

Result 1 The endemic steady states $E_{1,2}$ are locally asymptotically stable wherever they exist, that is, for all $R_i > 1$.

Proof. From local stability theory, a steady state is stable if it has negative eigenvalues. Since $K_{1,2} \geq 0$ because of Theorem 1, the proof trivially follows from the existence condition. □

We illustrate this result using a bifurcation where we arbitrarily choose $\alpha_9 = 0.762$ and $\kappa = 0.011$ in Figure 2.

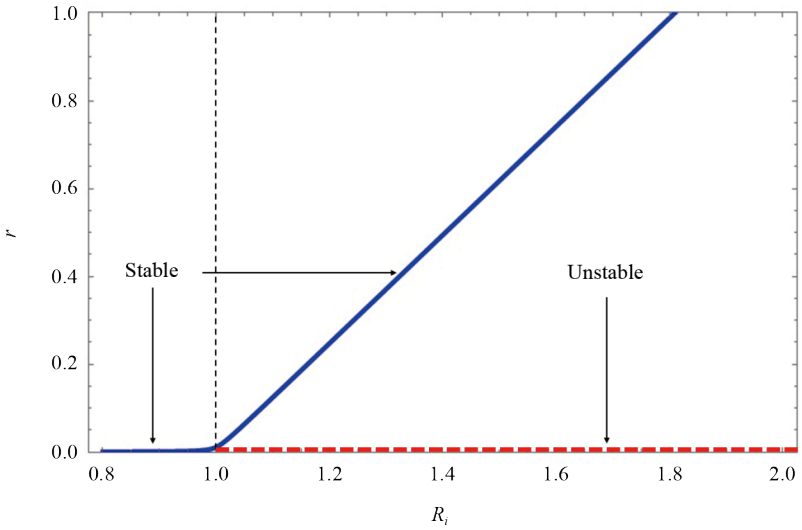

Figure 2. Model diagram indicative of a transcritical bifurcation

Figure 2 showed the Model diagram indicative of a transcritical bifurcation where two steady states (one stable and one unstable) merge and annihilate or emerge as R_i crosses a critical threshold $R_i = 1$.

Since the steady states $E_{1,2}$ are locally asymptotically stable for $R_i > 1$, the curve reflects stable steady states in this region. The shape and position of the curve help visualize how the stability changes and how the steady state evolves as R_i increases. There is an exchange of stability.

3. Simulations and results

In this section we approximate parameter values based on literature, calculations and reasonable estimates.

3.1 *Parameter estimation*

Due to lack of data, we present a hypothetical scenario to validate the model's assertions. At 85 dB, the probability of developing a significant hearing loss after a 40-year exposure is about 8-10% [14]. Exposure to 100 dB can cause immediate damage, with a safe exposure time of only 15 minutes (0.0104 days) to avoid permanent damage [15]. The rate of temporary threshold shift recovery varies, but a significant threshold shift can take days to weeks to recover, and permanent threshold shifts do not recover [16]. For temporary damage, recovery rate can be around 10-20 dB per day over the first few days after exposure, depending on the noise level and duration [17] and permanent damage is irreversible [18]. The parameter bounds for the model are defined based on several constraints: biological or physical limits, which ensure parameters stay within observed physiological ranges; conversion rates, which are set to non-negative values reflecting realistic transitions between different cell states; and noise intensity parameters, which are constrained to realistic limits for noise adjustment and response. We use the np.clip function from Python's NumPy library to adjust these values, ensuring that parameters do not exceed their expected ranges. We get the following hypothetical parameter values in Table 1.

Table 1. Table of description and values of parameters in the scaled model system

Parameter	Description	Value	Source
α_0	Hearing loss recovery index	0.01	Estimated
α_1	Relative recovery of hair cells given natural decay rate	0.01	Estimated
α_2	First level excess decay ratio	0.01	Estimated
α_3	First level impairment-incidence ratio	0.01	Estimated
α_4	Second level excess decay ratio	0.92	Estimated
α_5	Second level impairment-incidence ratio	0.75	Estimated
α_6	Maximum TTS factor due to maximum relative intensity	0.17	Estimated
α_7	Temporary Threshold factor	1	Estimated
α_8	TTS per level of intensity	0.762	Estimated

We use these values to simulate three baseline scenarios dependent on the level of sound intensity. This is followed by a sensitivity analysis of parameters on the state variable r.

3.2 *The baseline simulations*

We illustrate the baseline scenario in Figures 3-5. We show the dynamic behavior of the system described by the differential equations over time given high, medium and low sound intensities respectively, are all driven by α_8, the TTS per level of intensity. The graphs plot the values of the four variables u, v, w, and r against 200 time units starting from initial conditions $u(0) = 0.9$, $v(0) = 0.06$, $w(0) = 0.04$, $r(0) = 0$, showing the interplay and dynamic changes of these variables.

Figure 3 showed the time evolution of variables u, v, w, and r when $\alpha_6 = 0$. Healthy cells decrease to a steady state, but do not vanish. There are no fatigued or impaired hair cells as time increases.

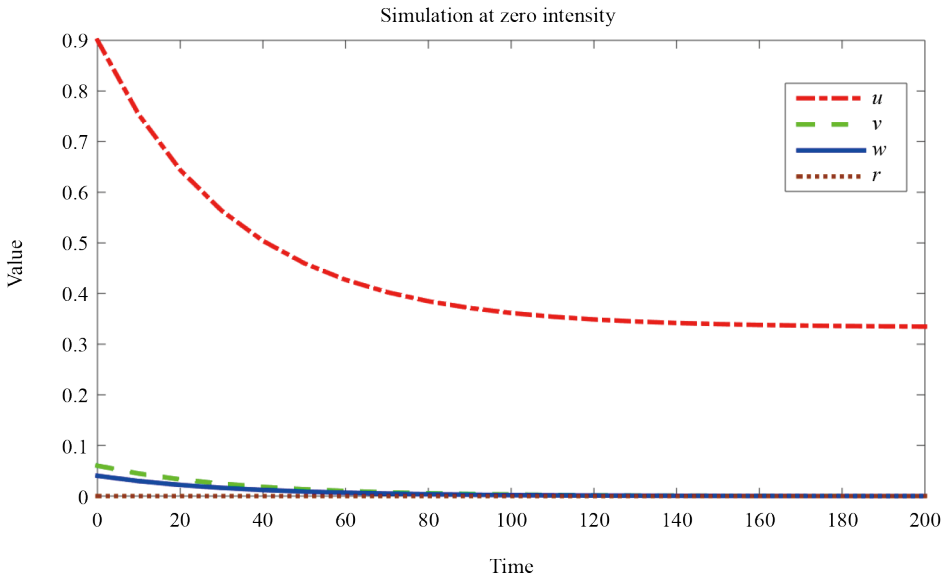

Figure 3. Time evolution of variables u, v, w, and r when $\alpha_6 = 0$

Figure 4 showed the time evolution of variables u, v, w, and r when $\alpha_6 = 0.17$. Healthy cells further decrease to a steady state, but do not vanish. There are fatigued and impaired hair cells as time increases.

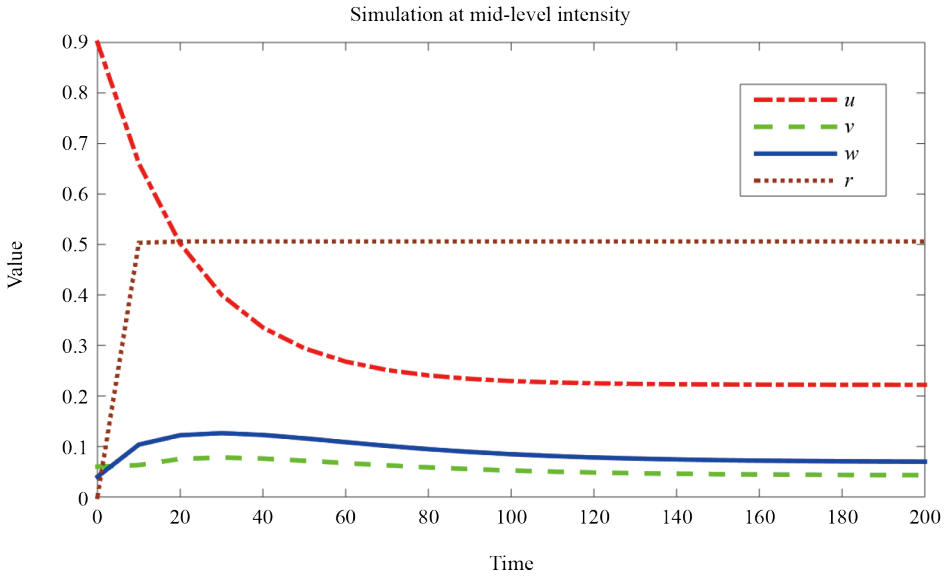

Figure 4. Time evolution of variables u, v, w, and r when $\alpha_6 = 0.17$

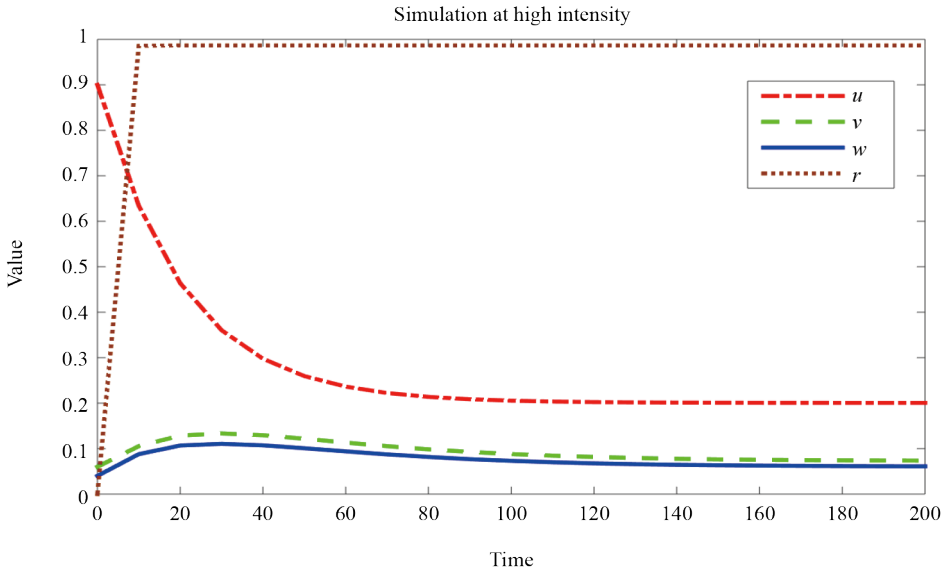

Figure 5. The number of fatigued hair cells and the number of damaged hair cells when $\alpha_6 = 0.49$

Figure 5 showed there is a level of intensity where the fatigued hair cells population increases more than the impaired high intensity with $\alpha_6 = 0.49$.

We start by establishing the effect of varying sound intensity in an environment. The baseline simulation in Figure 3 reveals that in the absence of sound intensity, that is $r = 0$, the healthy hair cells concentration u declines steadily to a steady state, and there are no unhealthy (fatigued or impaired) hair cells as times increases. The healthy hair cells population decreases further as r increases, and in Figure 4, the impaired hair cells population is greater than that of the

fatigued. A further increase in r shows no significant decline of the health hair cells concentration, and the fatigued hair cells population becomes greater than that of the impaired population as demonstrated in Figure 5.

3.3 *Sensitivity analysis with respect to sound intensity*

We conduct sensitivity analysis through Latin Hypercube Sampling (LHS) and Partial Rank Correlation Coefficient (PRCC) to identify key parameters influencing r. Parameters with the highest absolute PRCC values, whether positive or negative, are deemed critical and are the focus of subsequent simulations.

Figure 6 showed the plot illustrates how parameters are sensitive to the variable r using the initial values $u(0) = 0.9$, $v(0) = 0.06$, $w(0) = 0.04$, and $r(0) = 0.03$.

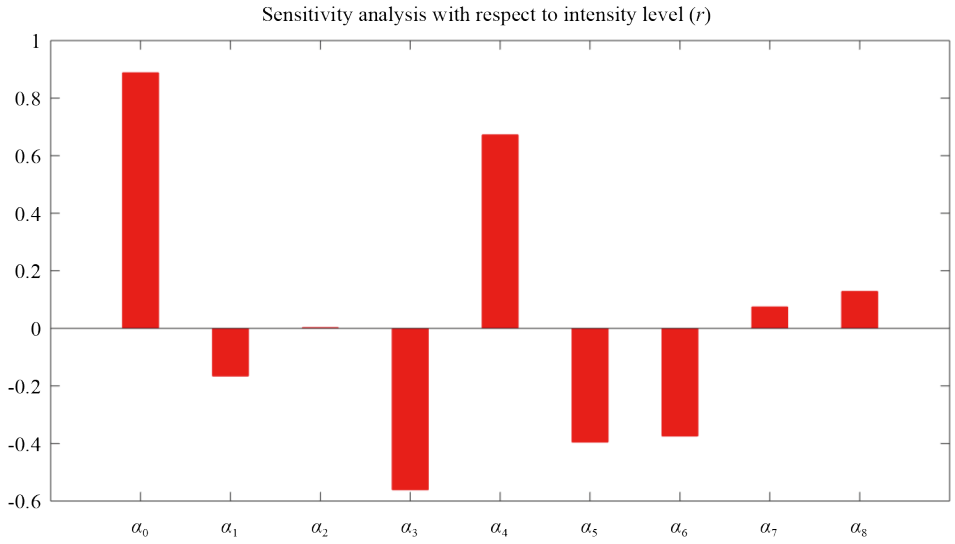

Figure 6. Sensitivity of the parameter to the variable r

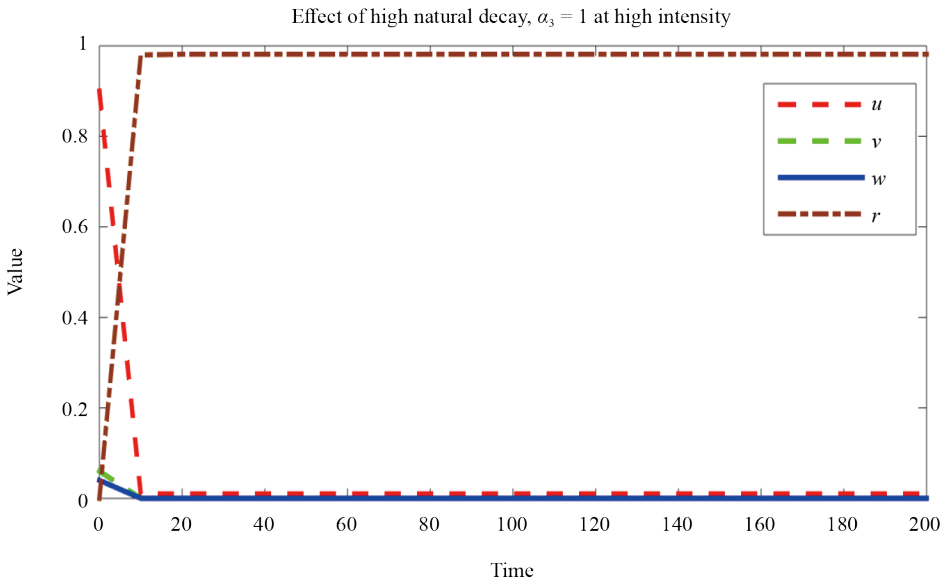

Figure 7. Time evolution of variables u, v, w, and r starting from initial conditions $u(0) = 0.9$, $v(0) = 0.06$, $w(0) = 0.04$, and $r(0) = 0.03$ when $\alpha_3 = 1$

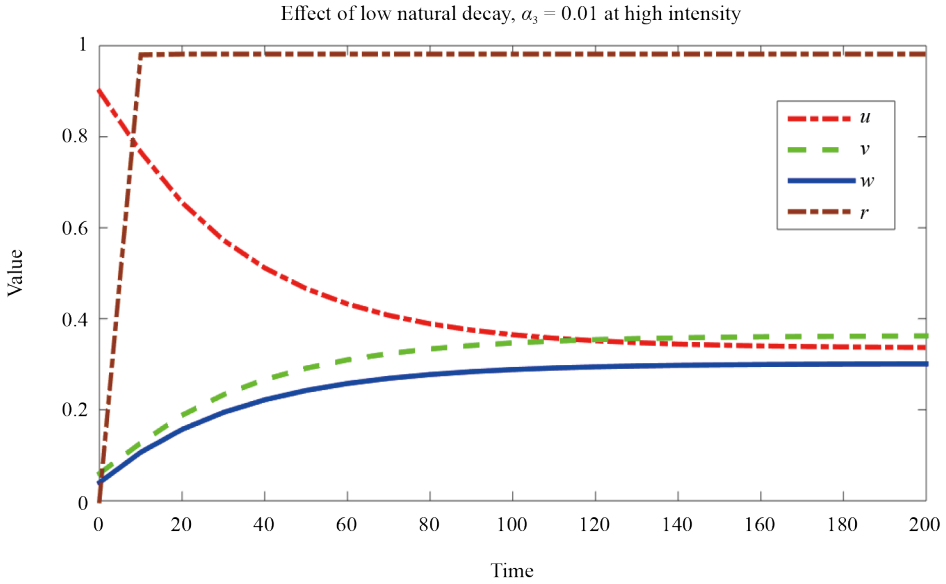

Figure 8. Time evolution of variables u, v, w, and r starting from initial conditions $u(0) = 0.9$, $v(0) = 0.06$, $w(0) = 0.04$, and $r(0) = 0.03$ when $\alpha_3 = 0.01$

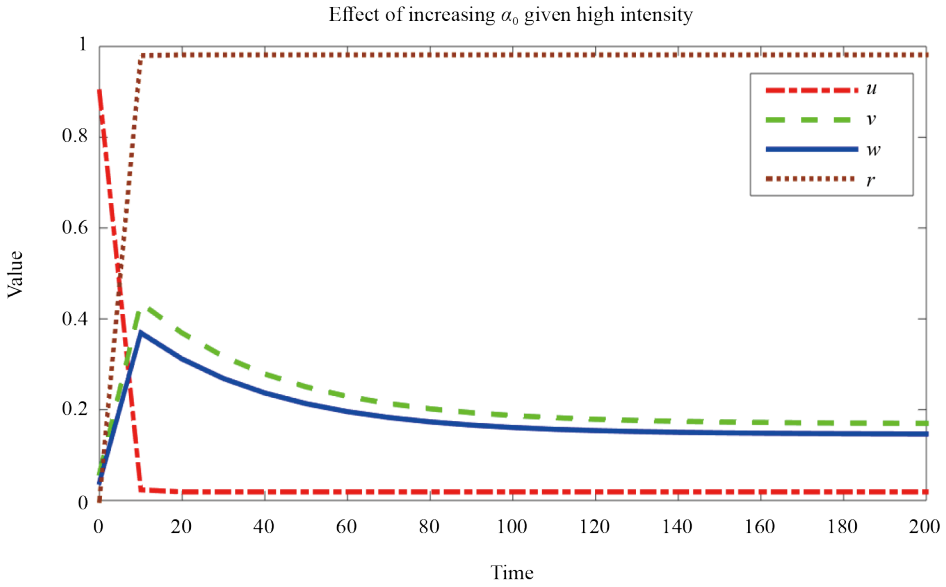

Figure 9. Time evolution of variables u, v, w, and r starting from initial conditions $u(0) = 0.9$, $v(0) = 0.06$, $w(0) = 0.04$, and $r(0) = 0.03$ when $\alpha_0 = 0.5$

The parameter α_3 has the highest negative PRCC values and the strongest negative influence on r. This means that as it decreases, r is likely to increase. The parameter α_0 has the highest positive PRCC values and the strongest positive influence on r. This means that as it increases, r is likely to increase as well. Equipped with these observations, in Figures 7-9, we vary α_3 over low-intensity levels. In Figure 7, given a high level of intensity ($r = 1$), if there is a high relative recovery of hair cells given a natural decay rate $\alpha_3 = 1$, then as much as the rate of return to baseline intensity is equal to the natural decay rate, the healthy population decreases to vanishing levels, just as the impaired population does. This is an indication of hearing loss thresholds. In Figure 8, we observe that if the sound intensity is at its maximum as in Figure 7, and there is a low relative recovery of hair cells given a natural decay rate $\alpha_3 = 0.01$, meaning that if the rate of return

to baseline intensity is greater than the natural decay rate, the healthy population decreases due to fatigue and the fatigued and impaired hair cell populations increase relative to the decline of the healthy hair cell population.

In Figures 9 and 10, we demonstrate the effect of varying the hearing loss recovery index α_0. At high intensity, as in the previous simulations, we observe that from the initial stages, there are more fatigued than impaired hair cells if $\alpha_0 = 0.5$. However, the healthy cell population vanishes, as is the case in Figure 10, because of a high rate of transition from the healthy cells to the impaired class. Hence, we observe more impaired hair cells than fatigued hair cells at high α_0 values and the notable vanishing of healthy cells.

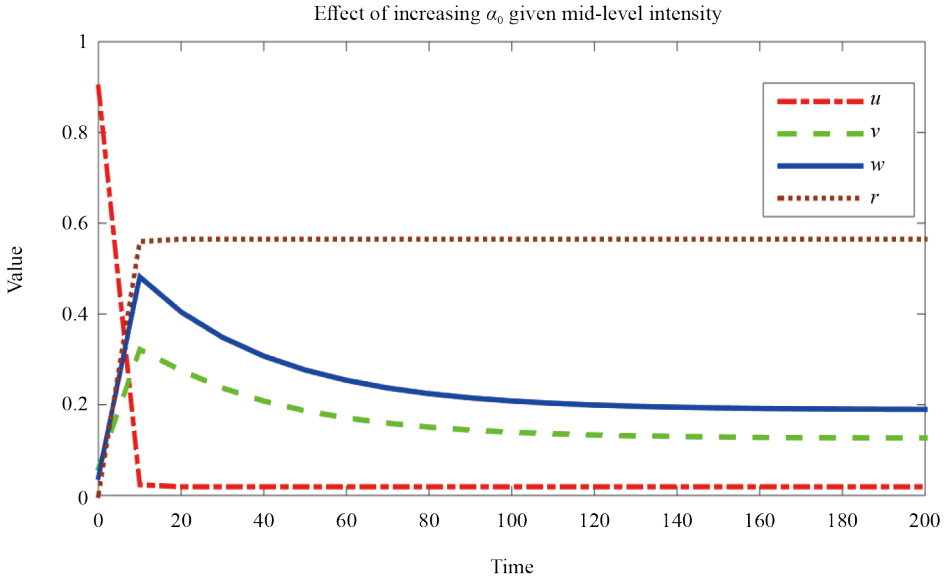

Figure 10. Time evolution of variables u, v, w, and r starting from initial conditions $u(0) = 0.9$, $v(0) = 0.06$, $w(0) = 0.04$, and $r(0) = 0.03$ when $\alpha_0 = 0.9$

3.3.1 *Summary of results*

We summarise the hearing loss dynamics focusing on both TTS and PTS in Table 2.

Table 2. Table of description and values of parameters in the scaled model system

Case	Influence on TTS or PTS
1. Low α_0, Low α_3, Low α_6	Extremely low TTS probability
2. Low α_0, Low α_3, High α_6	Moderately low TTS probability
3. Low α_0, High α_3, High α_6	High TTS probability
4. Low α_0, Highα_3, Low α_6	Low PTS probability
5. High α_0, Low α_3, Low α_6	High TTS probability
6. High α_0, Low α_3, High α_6	High TTS probability
7. High α_0, High α_3, Low α_6	Extremely high TTS probability
8. High α_0, High α_3, High α_6	Extremely high PTS probability

The drivers are α_0, which is good if it is low because intensity is forced to decrease to its baseline level; α_3, which is good if low because the number of hair cells lost from the hair cell population gets reduced (low chances of PTS); and α_6, which is good if low as well due to a reduced baseline intensity. From the hypothetical simulation in Figure 11, the green color shows safe levels, the yellow color denotes levels of exposure at which one must be cautious, and the red color represents dangerous levels that can lead to either TTS or PTS.

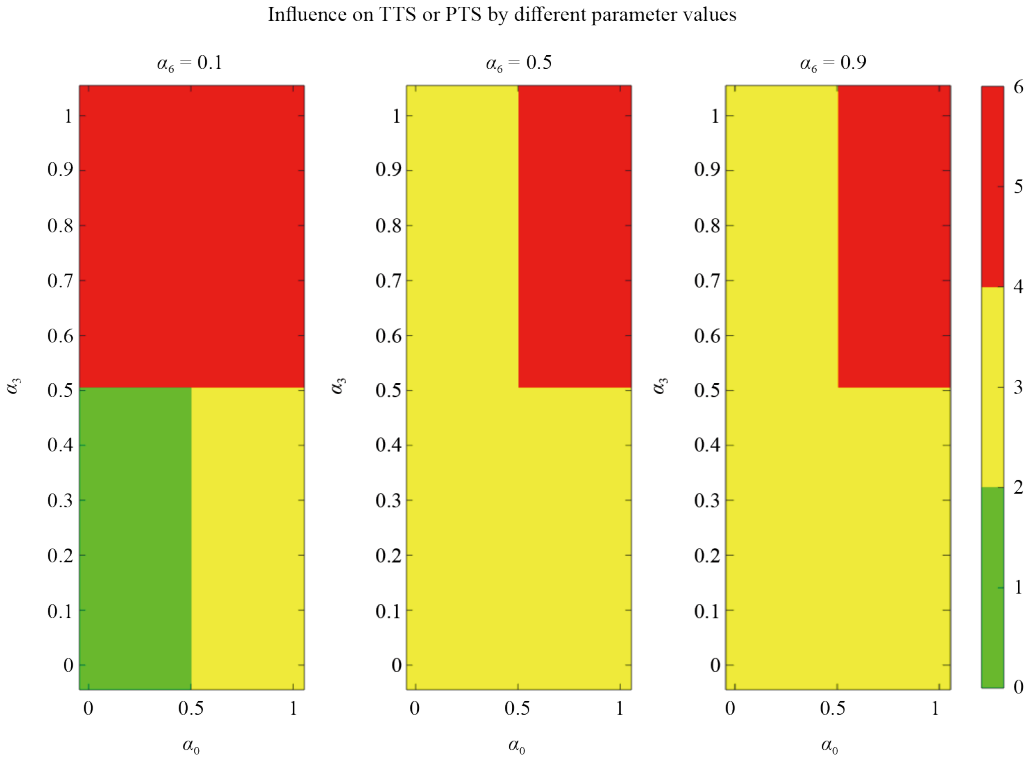

Figure 11. Illustrative heatmaps for different values of α_6 to visualize the possible outcomes (TTS or PTS) based on parameters α_0 and α_3

4. Discussion and conclusion

This study presents a mathematical modeling approach to quantifying the dynamics of cochlear hair cell populations under the influence of prolonged exposure to low-pressure sound, such as that encountered from the use of earphones. The aim of the study is to predict intervention points (at personal and global levels) to prevent hearing loss, as shown in Figure 11. The other purpose of this study is to establish instances of hearing loss, which are revealed through simulations. Scaling the model was essential since were dealing with two different quantities (hair cell population and intensity). It also enabled us to identify meaningful parameter groups used in the analysis.

The analysis of the system's steady states revealed the existence of two endemic equilibria, with local asymptotic stability dependent on surpassing a critical threshold of sound intensity. This suggests that there is a critical level of sound exposure above which the auditory system can no longer maintain a healthy state, leading to long-term hearing impairment. These findings are consistent with previous studies that have highlighted the adverse effects of chronic low-level noise exposure on auditory health [19, 20]. The identification of this critical threshold has important implications for public health policies, as it underscores the need for regulatory measures to mitigate the impact of high sound intensity on cochlear health and prevent long-term auditory damage.

The Jacobian matrix analysis of the system revealed the presence of a transcritical bifurcation, indicating transitions between stable and unstable states. This highlights the complex and nonlinear dynamics governing the response of hair

cells to sound exposure, and suggests that small changes in sound intensity can lead to dramatic shifts in the auditory system's state (see work in [21]). These insights contribute to a deeper understanding of the physiological mechanisms underlying Temporary Threshold Shift (TTS) and its potential progression to permanent hearing loss [22–24]. Simulation results in Figures 7, 8 and 9 show that for a given intensity level, hearing loss is inevitable for certain for specific Temporary Threshold Shift (TTS). Thus, we are able to quantify healthy and acceptable TTS levels, beyond which there are no healthy, fatigued or impaired hair cells. This creates a platform to measure the transition from healthy to unhealthy earphones uses.

Another key objective of this study answered by this undertaking is that of identifying or predicting instances of potential hearing loss. In Figures 3-5, we see that at high intensity the fatigued population exceeds the impaired population, which is reversed for mid-level intensity. This is an indication of a threshold shift facilitated by increasing the maximum TTS factor α_6, and evidenced by the slight decline in the healthy cells population when one compares Figures 4 and 5. Instances of potential hearing loss are further highlighted in Figure 11.

A key limitation of the current model is its assumption of uniform cochlear dynamics across all frequencies. The cochlea, however, has a tonotopic organization where different regions process different frequencies, with the base being more sensitive to high frequencies and the apex to low frequencies. This variation in sensitivity may affect the progression of Temporary Threshold Shifts (TTS) and permanent hearing loss differently across frequency ranges. Earphone-induced damage to cochlear hair cells is primarily driven by intensity but also has a frequency-dependent component. Loudness, measured in decibels, is the main factor contributing to hair cell damage. Sounds above 85 dB, particularly with prolonged exposure, can lead to temporary or permanent threshold shifts due to metabolic stress and eventual cell death in the cochlea [25]. Earphones pose a particular risk because they deliver sound directly into the ear canal, reducing natural dissipation and making it easier to exceed safe listening levels [11]. Frequency also plays a role, as the cochlea's tonotopic organization makes certain regions more vulnerable. High-frequency sounds are processed near the cochlear base, which is more susceptible to noise-induced damage. Since most music and speech fall within the mid-to-high frequency range (1-6 kHz), prolonged exposure to these frequencies at high intensity increases the risk of hearing loss [26]. High-frequency sounds at high intensity are particularly damaging because they exert greater mechanical stress on the cochlear base [27]. Since the model does not account for this frequency-dependent variation, it may limit its ability to accurately predict how noise exposure at different frequencies influences cochlear cell damage.

Other limitations include the simplifying assumptions made in the mathematical model, such as the lack of consideration for individual variability in hair cell regeneration and the influence of other factors like age and genetic predisposition. Additionally, the model does not account for the potential adaptive mechanisms the auditory system may employ to mitigate the effects of chronic low-level sound exposure. Despite these limitations, the results of this study have significant implications for researchers, clinicians, and the general public. For researchers in the field of auditory neuroscience and hearing health, the proposed mathematical framework offers a tool for predicting hearing impairment outcomes and guiding the development of evidence-based interventions. Clinicians can use the findings from this study to inform their understanding of the physiological processes underlying hearing loss and develop more effective prevention and treatment strategies. The general public, particularly those who frequently use earphones, can benefit from the study's findings by adopting safe listening practices and being more aware of the potential long-term consequences of prolonged exposure to low-pressure sounds.

Future work in the mathematical study of cochlear hair cell dynamics should incorporate individual variability, adaptive mechanisms, and stochastic elements to improve model accuracy and personalization. Integrating longitudinal data and optimizing intervention strategies can enhance predictive power and real-world applicability. While the current model provides valuable perspectives into the overall dynamics of cochlear health under sound exposure, the incorporation of tonotopic variation across frequencies would greatly enhance its realism and applicability to real-world auditory environments. Collaborative efforts with interdisciplinary experts and the development of educational tools will further support the prevention of hearing loss and promote safe listening practices.

Funding sources

This research did not receive any specific grant from funding agencies in the public, commercial, or not-for-profit sectors.

Authors' contributions

All authors contributed equally to the writing of this paper. All authors read and approved the final manuscript.

Conflict of interest

The authors declare that there is no conflict of interest regarding the publication of this paper.

References

[1] Natarajan N, Batts S, Stankovic KM. Noise-induced hearing loss. *Journal of Clinical Medicine*. 2023; 12(6): 2347. Available from: https://doi.org/10.3390/jcm12062347.

[2] Pienkowski M. Loud music and leisure noise is a common cause of chronic hearing loss, tinnitus and hyperacusis. *International Journal of Environmental Research and Public Health*. 2021; 18(8): 4236. Available from: https://doi.org/10.3390/ijerph18084236.

[3] Lie A, Skogstad M, Johannessen HA, Tynes T, Mehlum IS, Nordby KC, et al. Occupational noise exposure and hearing: a systematic review. *International Archives of Occupational and Environmental Health*. 2016; 89(3): 351-372. Available from: https://doi.org/10.1007/s00420-015-1083-5.

[4] Ryan AF, Kujawa SG, Hammill T, Le Prell C, Kil J. Temporary and permanent noise-induced threshold shifts: a review of basic and clinical observations. *Otology & Neurotology*. 2016; 37(8): e271-e275.

[5] Bannister S, Greasley AE, Cox TJ, Akeroyd MA, Barker J, Fazenda B, et al. Muddy, muddled, or muffled? Understanding the perception of audio quality in music by hearing aid users. *Frontiers in Psychology*. 2024; 15: 1310176. Available from: https://doi.org/10.3389/fpsyg.2024.1310176.

[6] Grossan M, Peterson DC. *Tinnitus*. StatPearls Publishing; 2023.

[7] Vielsmeier V, Kreuzer PM, Haubner F, Steffens T, Semmler PR, Kleinjung T, et al. Speech comprehension difficulties in chronic tinnitus and its relation to hyperacusis. *Frontiers in Aging Neuroscience*. 2016; 8: 293. Available from: https://doi.org/10.3389/fnagi.2016.00293.

[8] Daniel E. Noise and hearing loss: A review. *Journal of School Health*. 2007; 77(5): 225-231. Available from: https://doi.org/10.1111/j.1746-1561.2007.00197.x.

[9] Peng JH, Tao ZZ, Huang ZW. Risk of damage to hearing from personal listening devices in young adults. *Journal of Otolaryngology*. 2007; 36(3): 181-185.

[10] Torp L, Harms-Ringdahl K. Comparison of sound pressure levels in the ear canal with three different types of earphones. *International Journal of Audiology*. 2011; 50(3): 174-180.

[11] Fligor BJ, Cox LC. Output levels of commercially available portable compact disc players and the potential risk to hearing. *Ear and Hearing*. 2004; 25(6): 513-527.

[12] Levey S, Levey T, Fligor BJ. Noise exposure estimates of urban MP3 player users. *Journal of Speech, Language, and Hearing Research*. 2011; 54(1): 263-277. Available from: https://doi.org/10.1044/1092-4388(2010/09-0283).

[13] Wu PZ, O'Malley JT, de Gruttola V, Liberman MC. Age-related hearing loss is dominated by damage to inner ear sensory cells, not the cellular battery that powers them. *Journal of Neuroscience*. 2020; 40(33): 6357-6366. Available from: https://doi.org/10.1523/JNEUROSCI.0937-20.2020.

[14] Dobie RA, Humes LE. Noise-induced hearing loss in occupational settings. *Noise and Health*. 2002; 4(16): 1-22.

[15] National Institute for Occupational Safety and Health. *Criteria for a Recommended Standard: Occupational Noise Exposure, Revised Criteria 1998*. U.S. Department of Health and Human Services, Centers for Disease Control and Prevention, National Institute for Occupational Safety and Health; 1998.

[16] Canlon B, Illing RB, Zhu X. Stress and survival of cochlear hair cells. *Audiology and Neurotology*. 2007; 12(6): 379-388.

[17] Kujawa SG, Liberman MC. Adding insult to injury: cochlear nerve degeneration after 'temporary' noise-induced hearing loss. *Journal of Neuroscience*. 2009; 29(45): 14077-14085. Available from: https://doi.org/10.1523/JNEUROSCI.2845-09.2009.

[18] Humes LE, Wilson DL. Characterization of hearing loss due to noise exposure. *Journal of Speech, Language, and Hearing Research*. 2003; 46(4): 841-852.

[19] Kujawa SG, Liberman MC. Acceleration of age-related hearing loss by early noise exposure: evidence of a misspent youth. *The Journal of Neuroscience*. 2006; 26(7): 2115-2123. Available from: https://doi.org/10.1523/jneurosci.4985-05.2006.

[20] Śliwińska Kowalska M, Zaborowski K. WHO environmental noise guidelines for the European region: a systematic review on environmental noise and permanent hearing loss and tinnitus. *International Journal of Environmental Research and Public Health*. 2017; 14(10): 1139. Available from: https://doi.org/10.3390/ijerph14101139.

[21] Oxenham AJ. How we hear: the perception and neural coding of sound. *Annual Review of Psychology*. 2018; 69: 27-50.

[22] Dobie RA, Humes LE. Commentary on the regulatory implications of noise-induced cochlear neuropathy. *International Journal of Audiology*. 2017; 56(sup1): 74-78. Available from: https://doi.org/10.1080/14992027.2016.1255359.

[23] Humes LE. The World Health Organization's hearing-impairment grading system: an evaluation for unaided communication in age-related hearing loss. *International Journal of Audiology*. 2019; 58(1): 12-20. Available from: https://doi.org/10.1080/14992027.2018.1518598.

[24] Oishi N, Schacht J. Emerging treatments for noise-induced hearing loss. *Expert Opinion on Emerging Drugs*. 2011; 16(2): 235-245. Available from: https://doi.org/10.1517/14728214.2011.552427.

[25] Clark WW. Noise exposure from leisure activities: a review. *The Journal of the Acoustical Society of America*. 1991; 90(1): 175-181. Available from: https://doi.org/10.1121/1.401285.

[26] Dawes P, Fortnum H, Moore DR, Emsley R, Norman P, Cruickshanks K, et al. Hearing in middle age: a population snapshot of 40- to 69-year olds in the United Kingdom. *Ear and Hearing*. 2014; 35(3): e44-e51. Available from: https://doi.org/10.1097/AUD.0000000000000010.

[27] Fettiplace R, Kim KX. The physiology of mechanoelectrical transduction channels in hearing. *Physiological Reviews*. 2014; 94(3): 951-986. Available from: https://doi.org/10.1152/physrev.00038.2013.